1   **Insights into agricultural influences and weathering processes from major**

2   **ion patters in the Wiesent River catchment (Germany)**

3

4   Robert van Geldern[1],*, Peter Schulte[1,2], Michael Mader[1], Alfons Baier[1], Johannes A.C.

5   Barth[1], Kern Lee[1]

6

7   [1] *Friedrich-Alexander-University Erlangen-Nuremberg (FAU), Department of Geography*

8   *and Earth Sciences, GeoZentrum Nordbayern, Schlossgarten 5, 91054 Erlangen, Germany*

9   [2] *Gehrenhagweg 6, CH-5420 Ehrendingen, Switzerland*

10

11

12

13   for submission to

14   *Hydrological Processes*

15

16

17

18   *Corresponding author.

19   robert.van.geldern@fau.de. phone +49 9131 8522514. fax +49 9131 29294.

20

21

22 **ABSTRACT**

23 A study of the geochemical downriver evolution of the Wiesent River and its tributaries

24 revealed unexpected decreases of nitrate downstream from the source, with maximum values

25 of 31.6 mg L^{-1} to minimum values of 10 mg L^{-1} near the mouth. This trend persisted over the

26 length of the river even though increased agricultural activities are evident in the downstream

27 section of the catchment. This pattern is caused by fertilizer inputs via fast fracture flow and

28 fast conduits from karst lithology in the upstream area that may have reached the river's

29 source even from beyond the hydrological catchment boundaries. Further downstream, these

30 influences became diluted by tributary inputs that drain subcatchments dominated by

31 claystone and sandstone lithologies that increased potassium and sulfate concentrations. In

32 addition, except for inputs in the source area, groundwater contributions along the river

33 course were found to be minor as attested by seasonal temperature trends of the river, with

34 values ranging from 18.9 °C during summer to 0.9 °C during winter. This seasonality was

35 absent at the source where water temperatures were consistently 9 °C throughout the year,

36 which is a typical value for central European groundwater.

37

38 **KEYWORDS**

40

INTRODUCTION

41

42   The downriver evolution of various river systems has been examined in several studies

43   worldwide (Meybeck, 1982; Meybeck, 1993; Yang *et al.*, 1996; Richey *et al.*, 2002). Most of

44   these were aimed at weathering processes and continental fluxes of major element and carbon

45   phases. Following these studies, work on smaller river systems were also carried out (Barth *et*

46   *al.*, 2003; Kanduč *et al.*, 2007; Stögbauer *et al.*, 2008; Brunet *et al.*, 2011), and most of these

47   showed increasing conductivities and fluxes with closer proximity to confluences to larger

48   river systems. This trend corresponds to increasing element loads further downstream and is

49   usually related to increasing anthropogenic activities including traffic infrastructure,

50   settlements and agricultural practices in the downstream sections of catchments.

51   Here we present a small river system of 72.4 km length, the Wiesent River (Figure 1).

52   Being dominated by karst lithology, it was first studied as an ideal natural laboratory for

53   investigations of the aqueous carbon cycle in karst areas and its response to excessive carbon

54   loss to the atmosphere, particularly in its source area (van Geldern *et al.*, 2015). The

55   catchment is situated in a dolomite and calcite-dominated terrain that trends towards shale and

56   sandstone terrains in the lower reaches of the river. This allows for interpretations of spatial

57   heterogeneity in river water chemistry, while sampling over almost one year enabled temporal

58   interpretations of seasonal variations in riverine solutes, carbon transport, CO_2 evasion and

59   associated changes in the carbon isotope distribution of dissolved inorganic carbon (DIC).

60   The Wiesent River is also influenced by anthropogenic activities including farming, fish

61   farming and tourism. In particular, farming activities along the river course were expected to

62   significantly influence the water chemistry. These influences may be stronger in a karst-

63   dominated lithology as compared to catchments with clastic sediments, due to the fast conduit

64   systems present in karst. These conduits also make karst aquifers highly vulnerable to

65   anthropogenic pollution because of the virtual absence of filter effects that are common in

66   pore aquifers. Moreover, it is known that fertilizers can lower pH values and thus cause

67   additional weathering that should, in turn, be particularly pronounced in karst that is

68   susceptible to acidity changes (Perrin *et al.*, 2008; Gandois *et al.*, 2011).

69   The objectives of this study were to assess the spatial and temporal downriver evolution of

70   major ion chemistry in a typical karst river. Specifically, we investigated whether the

71   hypothesized continuous increase of solutes along the flow path of the river could be

72   observed. With this in mind, we evaluate relative influences of natural versus anthropogenic

73   impacts together with the role of groundwater contributions along the river course.

74   Disentangling the relative importance of these factors advance the understanding of source-

75   related inputs and at the same time, provide information on the dilution of anthropogenic and

76   weathering inputs in space and time. Regarding the high vulnerability of karst terrains by

77   agricultural land use and anthropogenic pollution, this is of particular interest with regard to

78   the ecological functioning of rivers with large proportions of limestone in their catchment

79   lithology.

80   **STUDY AREA**

81   The study area was located in southern Germany, in Northern Bavaria between the

82   cities of Bamberg, Bayreuth and Nuremberg (Figure 1). The total catchment area of the

83   Wiesent River is 1040 km^2. The source of the Wiesent River is located in the northwest of the

84   catchment area, at the hamlet of Steinfeld at 445 meters above sea level (m.a.s.l.). From this

85   point the river flows in a southeast to south direction. Near the town of Goeßweinstein, the

86   general flow direction changes westward until the river finally reaches the Regnitz River at

87   240 m.a.s.l. The total length of the Wiesent River is 72.4 km and the most important

88   tributaries are the rivers Kainach, Truppach, Puettlach, Aufsess, Leinleiter, and Trubach

4

89   (Figure 2). Two discharge gauges are located along the main river at the villages of Hollfeld

90   and Muggendorf. They show averaged long-term discharge values of 1.04 m^3 s^{-1} and 7.11 m^3

91   s^{-1}, respectively (LfU, 2014).

92   The study area is located in a karst region with lithologies of calcites and dolomites

93   that are occasionally interbedded with marly layers. These sediments form the Franconian

94   Jura uplands, which belong to the Franconian Alb that is part of the South German

95   Scarplands. Overall, late Jurassic carbonates cover the majority (~67%) of the catchment area

96   (Figure 2). These comprise a limestone sequence of up to 200 m thickness that is in part

97   dolomitized, and forms a typical karst landscape of the area with incised rivers and other dry

98   valleys, dolines and caverns. This carbonate sequence is overlain by relict patches of Late

99   Cretaceous sandstone with interbedded marl and shale layers.

100   All sedimentary layers dip at a shallow angle in an eastward direction. As a

101   consequence, lower Jurassic and Late Triassic sandstones and claystones that underlie the

102   thick Late Jurassic carbonate succession crop out in the south-western part of the catchment.

103   Additional sandstone and claystone lithologies of the same Triassic sequence also appear in

104   the eastern part of the main basin, in subcatchments of the tributaries Truppach and Puettlach.

105   Here, the sandstones and claystones were lifted to the surface along a northwest-southeast

106   striking fault.

107   The vegetation in the south-western part of the catchment is characterized by broad-leaved

108   forest dominated by beeches and scattered small fruit orchards. Coniferous trees largely forest

109   northern and central parts of the catchment, while the eastern regions consist of grassland

110   pastures. Numerous small villages are present in the basin and, particularly in the downstream

111   part of the catchment, agriculture plays an important role in land use.

112 **METHODS**

113   Eight locations (sites 1 to 8 in Figure 2) were sampled during eight field campaigns

114 between January and November 2010 in order to cover all seasons. Starting in April 2010, the

115 six most important tributaries were additionally sampled during the last six sampling

116 campaigns. All tributaries were sampled near their confluences with the Wiesent River (sites

117 9 to 14 in Figure 2), with water samples collected manually from the middle of the rivers. All

118 bottles were rinsed several times with sample water before filling. Samples destined for major

119 ion analyses were filled without headspace in double closure 100 mL high-density

120 polyethylene bottles with an inner stopper (product item LR100-2, Gosselin SAS, Borre,

121 France). These were then stored in the dark and at 4°C until analysis.

122 Measurements of temperature, pH, electrical conductivity (EC), and dissolved oxygen (DO)

123 were conducted in the field by a multi parameter instrument (WTW Multi 350i, WTW GmbH,

124 Weilheim, Germany). All probes were calibrated prior to each field campaign. The pH and

125 conductivity probes used built-in automatic temperature compensation functions, and

126 temperature precision is quoted as $\pm$ 0.1 °C by the manufacturer. Conductivity values were

127 referenced to 25 °C by a non-linear correction function (nLF) for natural waters. For pH

128 measurements precision was better than $\pm$ 0.05 pH units (1σ) and for conductivity

129 determinations it was better than $\pm$ 5 μS cm^{-1}. Dissolved oxygen was determined by a

130 galvanic sensor and automatically corrected for ambient air pressure by a built-in pressure

131 sensor.

132 Total alkalinity (TA) was determined from 100 mL water samples directly in the field by a

133 Hach Digital Titrator (Model 1690001, Hach Company, Loveland, CO, USA). The titration

134 endpoint was determined by colour changes of a pH indicator (bromcresol green-methyl red).

135 At a pH < 9, hydroxide (OH^{-}) does not contribute to TA at an appreciable concentration and

136   other TA contributing species (BOH_4^-, $H_3SiO_4^-$) can be regarded as negligible in the waters

137   examined by this study. Therefore, TA essentially contains only carbonic alkalinity and the

138   titration value was used for the calculation of carbonate species concentrations, which is

139   mainly bicarbonate (HCO_3^-) in the observed pH range (see Verma *et al.*, 2015)

140   Major cations (Na^+, K^+, Li^+, NH_4^+, Ca^{2+}, Mg^{2+}) and anions (F^-, Cl^-, NO_3^-, NO_2^-, SO_4^{2-}, PO_4^{3-})

141   were determined by ion chromatography (ICS 2000, Thermo Dionex, Sunnyvale, CA, USA).

142   Prior to ion chromatography analysis, samples were filtered with 0.45 μm disk filters, which

143   were flushed with sample before the autosampler vials were filled. Limit of quantification

144   (LOQ) for major ions was 0.1 mg L^{-1} with a typical precision of <5% (1σ) relative standard

145   deviation (RSD) based on the repeated analysis of two control standards treated as unknowns

146   in the lower and upper calibration range. Typical charge errors derived from equivalent

147   concentrations of ion chromatography and field titration data were between 5 and 12%.

148   **RESULTS**

149   *Major ion chemistry of the Wiesent River*

150   Major ion concentrations and the described trends along the river course are shown in

151   Figure 3. Detailed analytical data are available in the supplementary material to this article

152   from the website of the host journal, and are additionally archived in PANGAEA.[†]

153   Calcium showed the highest concentrations amongst all cations, followed by

154   magnesium, sodium, and potassium. Lithium concentrations were always below LOQ (<0.1

155   mg L^{-1}). Ammonium was detected in only two samples during February, with values of 0.11

[†] www.pangaea.de (DOI for data set pending)

156 and 0.28 mg L^{-1}, and was below the limit of detection (LOD) in all others. In contrast to most

157 other parameters, calcium and magnesium concentrations showed little variability at the

158 source during the various sampling campaigns, although their general downstream patterns

159 were almost identical for all sampling campaigns. Calcium exhibited a range of 90 to 145 mg

160 L^{-1}, whereas magnesium concentrations ranged between 15 and 45 mg L^{-1} (Figure 3).

161 Calcium concentrations showed an initial decrease between the source and sampling site 2,

162 whereas magnesium increased within the same direction. Further downstream, calcium

163 concentrations remained fairly stable and ranged between 105 and 130 mg L^{-1}, with exception

164 of the November campaign that was characterized by lower values further downstream. After

165 the initial rise, magnesium concentrations tended to decrease until sampling site 4 and showed

166 only minor variations thereafter. In particular, magnesium concentrations showed a clear

167 correlation with corresponding conductivity values for different sampling campaigns, which

168 in turn were correlated with precipitation events and resulting increased discharge values

169 (data shown in van Geldern *et al.*, 2015). This trend was also obvious to a lower extent for

170 calcium, especially during the November campaign.

171   Sodium concentrations ranged from 8 to 15 mg L^{-1}, stabilizing at a value of 11.2

172 (±0.6) mg L^{-1} at the source followed by a slight initial rise [arithmetic average (±1σ)]. Values

173 declined further downstream to concentrations of about 8 mg L^{-1} at the lower river course.

174 Potassium concentrations increased from 1.04 (±0.24) mg L^{-1} at the source to values of

175 around 2.0 mg L^{-1} downriver. Maximum values of 3.5 mg L^{-1} were recorded during the

176 November sampling campaign at site 4 and also at locations further downstream. Note that

177 during this campaign most other parameters, as for example calcium and magnesium

178 concentrations or conductivity, showed lower values, a trend that was most likely related to

179 heavy rains prior to that campaign.

180   The ranking of anions in order of decreasing concentrations at the Wiesent River

181   source was bicarbonate, nitrate, chloride, and sulfate with concentrations of 357 ($\pm$7), 29.6

182   ($\pm$2.7), 22.7 ($\pm$1.6), and 15.8 ($\pm$1.5) mg L^{-1}, respectively. Interestingly, the downstream

183   behavior revealed different patterns for these anions. Nitrate showed an almost linear

184   monotonic decline over the river course to 17.6 ($\pm$1.6) mg L^{-1} at the final sampling site and

185   bicarbonate decreased to an average of 307 ($\pm$22) mg L^{-1}. The lowest bicarbonate values were

186   measured along the lower course during the November sampling campaign. A pronounced

187   decrease was observed after the confluence with the Truppach, whereby bicarbonate

188   concentrations dropped below 250 mg L^{-1} in November. The minimum concentration of 228

189   mg L^{-1} was recorded at site 6, located downstream of the Puettlach tributary. During other

190   campaigns, bicarbonate concentrations along the lower course (site 4 and downstream),

191   ranged from 340 to 280 mg L^{-1} (Figure 3).

192   The chloride downstream evolution was similar to sodium or magnesium, with a

193   distinct increase from the source to sampling site 2 and subsequent decreasing values.

194   Chloride concentrations along the lower course ranged from 15 to 25 mg L^{-1}. In contrast,

195   sulfate behaved similar to potassium with a continuous increase along the Wiesent River up to

196   values of 20 to 30 mg L^{-1} near the mouth of the Wiesent at its confluence to the Regnitz. A

197   larger variability of sulfate could be observed downstream of sampling site 4. Here, maximum

198   concentrations of up to 42 mg L^{-1} were recorded during the November sampling campaign.

199   However, an exception from this behavior was observed in February, when the second highest

200   sulfate concentrations were measured at the middle and lower course while the downstream

201   conductivity curve showed maximum values (Figure 3).

202   Low concentrations for fluoride and phosphate above LOD were detected in 12 and 11

203   out of 64 analyses, respectively. When detected, typical concentrations of F^{-} and PO$_4^{3-}$ were

9

204 below 0.3 mg L^{-1} and never exceeded 0.5 mg L^{-1}. Nitrite was not detected in any of the

205 sampling campaigns in the main stem of the Wiesent River (cf. supplementary material)

206   The tributary and Wiesent River samples are characterized by their major ions in a

207 Piper diagram (Figure 4). Here the tributaries are marked with their numbers in brackets

208 according to Figure 2. The tributaries Kainach (9), Aufsess (11), and Trubach (14) were

209 largely similar to the water chemistry of the main stem of the Wiesent River. The only

210 exception was the Leinleiter tributary (13) with its lower magnesium concentrations, but most

211 other major ion concentrations were similar to those in the main river. Note that the two

212 eastern tributaries Truppach (10) and Puettlach (12) plot differently in Figure 4. For instance,

213 magnesium concentrations were below 12 mg L^{-1} in all samples taken from the Truppach

214 tributary. Morover, both the Truppach and the Puettlach, were characterized by lower

215 bicarbonate, increased potassium, and high sulfate concentrations. These patterns were also

216 transferred to the middle and lower course of the Wiesent River. This was particularly evident

217 after precipitation events, for instance during November. Finally, low concentrations of

218 phosphate (0.11 to 0.72 mg L^{-1})were found during all campaigns in the Truppach and

219 Puettlach, but not in the other tributaries.

220 **DISCUSSION**

221 *Geological and anthropogenic controls*

222   The downstream evolution of the parameters discussed above indicates that

223 groundwater is one of the major contributors to the Wiesent River and its tributaries. The

224 expectation is that groundwater infiltration to the river occurs primarily by the piston-flow

225 effect and minor contributions should be derived from overland runoff or soil water. The

226 latter processes are normally observed during snowmelt and more intensive precipitation

227 events. This would particularly hold true for precipitation in tributaries that drain poorly

10

228 permeable sediments such as in the eastern part of the catchment (i.e., Truppach and

229 Puettlach). Mixing of these tributary waters with the main river is the most important process

230 for dilution of total dissolved solids (TDS), as indicated by lower conductivity values. In

231 contrast, in the upstream part of the Wiesent Catchment, runoff generation should play a more

232 important role than in permeable karst lithology with fast infiltration rates.

233   When tributaries are chemically different as compared to the main stem of the Wiesent

234 River, their influences are expected to be obvious. For instance, lower magnesium

235 concentrations in the Truppach likely caused the pronounced drop in magnesium after

236 sampling sites 3 in the Wiesent River. This decline was even more pronounced during periods

237 of low conductivity after precipitation events.

238   On the other hand, contributions of tributaries that drain a similar lithology as the

239 Wiesent River are harder to detect by natural tracers. For instance, near the catchment outlet,

240 the lithology along the Wiesent River valley changes from carbonate rocks to claystone. The

241 formation is known as the Feuerletten Formation from the Late Trassic. Except for small

242 changes in calcium, magnesium, and sodium the measured parameters did not respond to this

243 prominent change in riverbed lithology. This indicates that groundwater contributions at the

244 final river stretch likely become less important due to the less permeable nature of the

245 underlying thick claystone formation.

246   At the source of the Wiesent, Ca^{2+}, Mg^{2+}, and HCO_3^- account for 86 % of the TDS and

247 along the river course, this value varies only slightly between 81 and 88 %. This shows that

248 carbonate weathering of calcite ($CaCO_3$) and dolomite ($CaMg(CO_3)_2$) mainly accounts for the

249 high concentrations of these three ions. The stoichiometry of carbonate weathering reactions

250 demands that carbonate-derived calcium and magnesium should be equal to those of

251 bicarbonate when expressed in (milli)equivalents per liter (meq/L). Such a plot of HCO_3^-

252　versus ($Ca^{2+} + Mg^{2+}$) concentrations reveals a general excess of calcium plus magnesium over

253　bicarbonate (Figure 5A). This excess of cations is partially balanced by Cl^-, SO_4^{2-} and NO_3^-,

254　and suggests that fractions of calcium or magnesium concentrations in the watershed were not

255　exclusively derived from carbonate weathering. Other potential natural sources of calcium are

256　gypsum or silicate weathering of Ca-bearing minerals such as anorthite. However, both

257　minerals are of minor importance in the Jurassic limestone formations and are therefore

258　unlikely candidates for leaching Ca^{2+} and Mg^{2+}.

259　　　　Other sources for this excess include mineral fertilizers that may contain calcium- or

260　magnesium-bearing compounds. This should also correlate with other solutes that are

261　typically derived from these fertilizers, such as nitrate. Further anthropogenic sources that

262　may exist in the watershed include organic fertilizers or domestic sewage. Typical

263　anthropogenic compounds are phosphate, sulfate and nitrogen compounds (NO_3^-, NO_2^-, NH_4^+)

264　from manure and mineral fertilizers. In particular, elevated nitrate concentrations are often

265　related to the use of such fertilizers. During this study, the highest concentrations of nitrate

266　were found at the source of the Wiesent River with a stable value of 29.6 (±2.7) mg L^{-1}. This

267　stability of nitrate concentrations at the source suggests that nitrate may have been

268　continuously transferred into the feeding karst aquifer that acted as a large reservoir.

269　Subsequently, nitrate likely has accumulated over decades and seasonal variations became

270　negligible.

271　　　　This supports the interpretation that the observed excess of calcium and magnesium is

272　a result of long-term anthropogenic influences on the groundwater, particularly at the Wiesent

273　River spring and the upper reaches. It thus indicated the influences from farming activities in

274　the upper part of the catchment. This is surprising, because the Wiesent River has its source in

275　a rural, largely natural region where forests dominate large portions of the catchment and

276   industry does not play a significant role. Therefore, anthropogenic signals in river water

277   chemistry were expected to be minimal, with inorganic aquatic chemistry mainly mirroring

278   weathering processes or changes in lithology. However, particularly in karst systems,

279   anthropogenic influences may directly enter the river via fast conduit systems and fracture

280   flow.

281   As opposed to the expected trend of increasing nitrate concentrations further

282   downstream where agriculture and urbanization is more prevalent, a contrary pattern was

283   observed: nitrate concentrations were found to be highest at the source of the Wiesent River

284   (see discussion above) and subsequently decreased with distance from the headwaters during

285   all sampling periods (Figure 3). This pattern further suggests the long-term influences of

286   agricultural land use on the groundwater, particularly in the upstream part of the watershed.

287   Even though agricultural activities are also prevalent in the downstream part of the catchment,

288   their associated nitrate releases may not reach the river as rapidly because the lithology

289   contains a high proportion of fine sandstones and shales that slows or hampers groundwater-

290   related transport to the river.

291   As for other anthropogenic parameters, road salt and domestic sewage are a primary

292   source of sodium and chloride. Increases in chloride or sodium concentrations were not

293   observed at the source during colder periods. This could either mean that they were dampened

294   in the large feeding karst reservoir or that road salting had a minor influence on the river

295   water chemistry. Since both chloride and potassium showed no distinct seasonality over the

296   entire course or the river, a pronounced influence of this source is likely small in this

297   catchment. It is more likely that these elements reach the river via agricultural activities that

298   are more dominant in the source region, as previously stated. At this juncture, it is unclear

299   why both Cl^- and Na^+ show significant increases from the spring to the second sampling

13

300   station (site 2) although this trend may be related to the presence of point sources such as

301   sewage release from private housing or farms.

302   Cl^- was also found to be in excess of Na^+ and K^+ and their cation-anion plot does not follow a

303   1:1 ratio (Figure 5B). The Cl^- excess could in part be balanced by excess Ca^{2+} and Mg^{2+} that

304   does not account for carbonate weathering. When assuming that this cation excess stems from

305   fertilizer use in the upstream part of the catchment, it supports the hypothesis that fertilizers

306   are more pronounced in upstream section and may have entered the river via fracture flow of

307   the present karst system.

308   Other fertilizers derived from potash with compounds such as KCl or K_2SO_4 may also

309   have added to the fertilizer load of the river. However, both K^+ and SO_4^{2-} have their lowest

310   values in the source region and show increases further downstream. At first sight, this pattern

311   does not appear to support the hypothesis of more pronounced fertilizer input in the upstream

312   part of the catchment. However, it is possible that both ions actually enter the river as a result

313   of fertilizer transport in the upstream, karst-dominated section of the catchment. The baseline

314   values at the source may then have increased further downstream mainly as a result of K^+ and

315   SO_4^{2-} released from weathering processes in the clay-rich shale formations in the eastern

316   subcatchments, and discharged into the main river stem via tributaries. These and other

317   mechanisms of tributariy influences are discussed in the following section.

318   *Downstream geochemical evolution*

319   After setting of the initial values for physico-chemical parameters at the source, many

320   parameters show changes along the river course. This may be either related to processes that

321   occur within the main river itself such as seasonal temperature changes, or due to the inflow

322   and mixing of waters from different sources.

323   An important question in river research is the interaction between river water and

324   surface water within the hyporheic and riparian zones along the river course (Krause *et al.*,

325   2009; Krause *et al.*, 2014). Depending on the hydraulic system, the river can lose water to the

326   groundwater by outflow through the riverbed. This situation is denoted as a losing stream.

327   Alternatively, water from the riparian zone can feed the river, which is denoted as a gaining

328   steam. Different environmental tracers, for example temperature, stable isotopes, or

329   wastewater-related pollutants, have been used to investigate these interactions in detail

330   (Engelhardt *et al.*, 2014; Fox *et al.*, 2016). Furthermore, tributaries with different water

331   chemistry that mix with the main river can also induce changes in water chemistry when

332   differences and fluxes are large enough to cause a measurable shift.

333   The downstream temperature development of the Wiesent River varies seasonally,

334   with higher temperatures in summer and lower temperatures in winter (Figure 3).

335   Groundwater seeps would shift the warm or cold temperature curve locally towards the

336   average groundwater temperature of about 9 ° C for this region. However, the spatial

337   resolution along the river is not detailed enough to detect point-source groundwater inflow.

338   This is because groundwater temperature can be expected to adjust quickly to the temperature

339   of the river water. Small groundwater contributions would therefore only be detectable close

340   to the point of inflow. However, a steady and spatially ubiquitous groundwater inflow along

341   the whole river course would likely dampen the seasonal changes of the river. Such trends

342   could only be observed at the source and for the remainder of the river it is more likely that

343   groundwater contributions are of minor importance.

344   A closer examination of the downstream curves showed a notable increase in

345   magnesium concentrations of 7 to 13 mg L^{-1} from the source to sampling site 2 (Figure 3). A

346   larger fraction of dolomite weathering might have increased the portion of magnesium over

347   calcium. However, this shift was also correlated with increases of sodium and chloride. To a

348   large degree, both elements are likely of anthropogenic origin and this pattern suggests that

349   the Mg^{2+} increase has an anthropogenic component. This is supported by the fact that the

350   increase in chloride was larger than the corresponding increase in sodium, so that chloride

351   could have additionally buffered the magnesium increase. However, even when accounting

352   for Cl^-, a negative charge deficit persisted and Mg^{2+} must have been additionally balanced by

353   other anions. As no other major anions (SO_4^{2-}, NO_3^-) showed a corresponding increase, the

354   surplus of magnesium is most likely buffered by organic compounds that were not measured

355   in this study.

356   Potassium and sulfate downstream evolutions in the Wiesent River showed opposing

357   patterns as compared to the other major ions along the course (see above). Both ion

358   concentrations gradually increased downstream, whereas other major ion concentrations

359   decreased most likely due to dilution effects by the tributaries Truppach and Puettlach that

360   drain a different lithology. Their lithology is dominated by claystone and sandstone (see

361   Figure 2) and increased concentrations of potassium and sulfate were observed in these two

362   eastern tributaries (supplementary material). A potential anthropogenic source could be

363   potassium sulfate, a common inorganic fertilizer that is often used in fruit orchards. Both ions

364   show a fairly strong correlation in the two subcatchments (Pearson correlation coefficient $r =$

365   0.69, $p = 0.012$) but only about one-tenth of the sulfate is balanced by potassium in this

366   scenario.

367   One plausible natural source for potassium is weathering of orthoclase and other

368   potassium-bearing silicate minerals in the clastic sediments. As a result of these weathering

369   processes, higher potassium concentrations may have been transported into the Wiesent

370   River.

371   The higher sulfate concentrations could have been caused by the dissolution of

372   gypsum and/or weathering of pyrite. Both minerals are present in the Lower and Middle

373   Jurrasic formations (Krumbeck, 1956; Schröder, 1968) and pyrite is especially abundant in

374   the thick claystone sequence of the 'Amaltheenton' and 'Opalinuston' formation that cover

375   large areas of the eastern subcatchments (Wippern, 1955). The principles of pyrite oxidation

376   follow a sequence of reactions that involve microbiologically-mediated and oxic

377   decomposition of pyrite followed by an anoxic decomposition of pyrite by ferric iron

378   (Lowson, 1982; Evangelou, 1995). The overall stoichiometry is represented by

$$2FeS_2 + 7O_2 + 2H_2O \rightarrow 2Fe^+ + SO_4^{2-} + 4H^+. \tag{1}$$
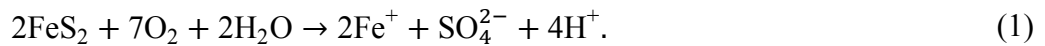
379   Pyrite weathering reactions release acidity and result in low pH values. However, lower pH

380   values were neither observed in the Wiesent nor in any of the tributaries. This absence of

381   expected pH decrease could be explained by the presence up to 10% carbonates in the

382   claystones (Schröder, 1968). This means that acidity derived from equation (1) could become

383   directly neutralized by reaction with carbonates.

384   Unexpectedly higher concentrations of potassium and sulfate in the Truppach and

385   Puettlach tributaries was observed in November: samples from this month showed increased

386   concentrations of potassium and sulfate that were also found in the middle and lower reaches

387   of the Wiesent River, downstream of the Truppach and Puettlach confluences (Figure 3). In

388   contrast, most other ions (e.g., calcium or magnesium) were diluted. This dilution can be

389   attributed to increased fluxes of low-mineralized surface runoff following a heavier period of

390   rainfall in November. Surface runoff was also expected to also dilute the concentrations of

391   potassium and sulfate. However, the data suggest that potassium and sulfate were largely

392   derived from weathering processes at the land surface or in the soil zone. They were then

393   mobilized and flushed with increased concentrations along the eastern tributaries into the

394   Wiesent River during precipitation events.

CONCLUSIONS

396   The Wiesent River has an unusual chemical downriver evolution, particularly for

397   solutes that are often derive from agricultural fertilizers. While increased anthropogenic

398   activities normally occur in the downriver sections of the catchment, an unexpectedly stronger

399   fertilizer-derived signal was found in its upstream area. This is particularly true for nitrate.

400   These agricultural inputs may have been introduced through fast conduit and fracture flow in

401   the karst lithology of the upstream catchment. Agricultural influences may even stem from

402   beyond the catchment surface water boundaries. After leaving the source, these inputs became

403   diluted further downstream, specifically via tributaries that were not sourced from carbonate

404   lithologies. While Ca^{2+}, HCO_3^- and NO_3^- decreased over the course of the river, we found

405   increases of K^+ and SO_4^{2-} in the downstream section that is more influenced by clay

406   lithologies. This enables a division of the river into two sections: an upstream part that is

407   dominated by karst and receives strong fertilizer inputs, and a downstream section that

408   receives less groundwater inputs but is subject to increased contributions by tributaries that

409   drain sandstone and shale lithologies. This highlights the importance of including tributaries

410   in river studies.

411   Overall, our findings indicate that bedrock geology remains the dominant control on

412   the major ion chemistry of the Wiesent River, and that agricultural influences are the

413   strongest near the headwaters despite increased land-use further downstream, due to long-

414   term storage and accumulation in karst aquifers. Future studies should include ecological

415   indicators that may be more sensitive to fertilizer input, such as counts of specific organisms

416   and quantification of sediment loads.

417

426

427

428   **References**

429   Barth JAC, Cronin AA, Dunlop J, Kalin RM. 2003. Influence of carbonates on the riverine

430   carbon cycle in an anthropogenically dominated catchment basin: Evidence from

431   major elements and stable carbon isotopes in the Lagan River (N. Ireland). *Chemical*

432   *Geology* **200**: 203-216.

433   Brunet F, Potot C, Probst A, Probst JL. 2011. Stable carbon isotope evidence for nitrogenous

434   fertilizer impact on carbonate weathering in a small agricultural watershed. *Rapid*

435   *Communications in Mass Spectrometry* **25**: 2682-2690. DOI: 10.1002/rcm.5050.

436   Engelhardt I, Barth JAC, Bol R, Schulz M, Ternes TA, Schüth C, van Geldern R. 2014.

437   Quantification of long-term wastewater fluxes at the surface water/groundwater-

438   interface: An integrative model perspective using stable isotopes and acesulfame.

439   *Science of the Total Environment* **466-467**: 16-25. DOI:

440   10.1016/j.scitotenv.2013.06.092.

441   Evangelou VP. 1995. *Pyrite oxidation and its control*. CRC Press; 293.

442   Fox A, Laube G, Schmidt C, Fleckenstein JH, Arnon S. 2016. The effect of losing and

443   gaining flow conditions on hyporheic exchange in heterogeneous streambeds. *Water*

444   *Resources Research* **52**: 7460-7477. DOI: 10.1002/2016WR018677.

445   Gandois L, Perrin A-S, Probst A. 2011. Impact of nitrogenous fertiliser-induced proton

446   release on cultivated soils with contrasting carbonate contents: A column experiment.

447   *Geochimica et Cosmochimica Acta* **75**: 1185-1198. DOI: 10.1016/j.gca.2010.11.025.

448   Kanduč T, Szramek K, Ogrinc N, Walter L. 2007. Origin and cycling of riverine inorganic

449   carbon in the Sava River watershed (Slovenia) inferred from major solutes and stable

450   carbon isotopes. *Biogeochemistry* **86**: 137-154. DOI: 10.1007/s10533-007-9149-4.

451   Krause S, Boano F, Cuthbert MO, Fleckenstein JH, Lewandowski J. 2014. Understanding

452   process dynamics at aquifer-surface water interfaces: An introduction to the special

453   section on new modeling approaches and novel experimental technologies. *Water*

454   *Resources Research* **50**: 1847-1855. DOI: 10.1002/2013WR014755.

455   Krause S, Hannah DM, Fleckenstein JH. 2009. Hyporheic hydrology: interactions at the

456   groundwater-surface water interface. *Hydrological Processes* **23**: 2103-2107. DOI:

457   10.1002/hyp.7366.

458   Krumbeck L. 1956. *Erläuterungen zur Geologischen Karte von Bayern 1: 25000 - Blatt Nr.*

459   *6232 Forchheim*. Bayerisches Geologisches Landesamt; 80.

460   LfU. 2014. Hochwassernachrichtendienst. Bayerisches Landesamt für Umwelt (LfU).

461   Accessible at http://www.hnd.bayern.de, (last accessed 28 Feb 2014).

462   Lowson RT. 1982. Aqueous oxidation of pyrite by molecular oxygen. *Chemical Reviews* **82**:

463   461-497. DOI: 10.1021/cr00051a001.

464   Meybeck M. 1982. Carbon, nitrogen, and phosphorus transport by world rivers. *American*

465   *Journal of Science* **282**: 401-450. DOI: 10.2475/ajs.282.4.401.

466   Meybeck M. 1993. Riverine transport of atmospheric carbon: Sources, global typology and

467   budget. *Water, Air, and Soil Pollution* **70**: 443-463. DOI: 10.1007/BF01105015.

468   Perrin A-S, Probst A, Probst J-L. 2008. Impact of nitrogenous fertilizers on carbonate

469   dissolution in small agricultural catchments: Implications for weathering CO2 uptake

470   at regional and global scales. *Geochimica et Cosmochimica Acta* **72**: 3105-3123.

471   DOI: 10.1016/j.gca.2008.04.011.

472   Richey JE, Melack JM, Aufdenkampe AK, Ballester VM, Hess LL. 2002. Outgassing from

473   Amazonian rivers and wetlands as a large tropical source of atmospheric CO2.

474   *Nature* **416**: 617-620.

475   Schröder B. 1968. *Erläuterungen zur Geologischen Karte von Bayern 1:25000 - Blatt Nr.*

476   *6332 Erlangen Nord*. Bayerisches Geologisches Landesamt; 159.

477   Stögbauer A, Strauss H, Arndt J, Marek V, Einsiedl F, van Geldern R. 2008. Rivers of North-

478   Rhine Westphalia revisited: Tracing changes in river chemistry. *Applied*

479   *Geochemistry* **23**: 3290-3304. DOI: 10.1016/j.apgeochem.2008.06.030.

480   van Geldern R, Schulte P, Mader M, Baier A, Barth JAC. 2015. Spatial and temporal

481   variations of pCO$_2$, dissolved inorganic carbon and stable isotopes along a temperate

482   karstic watercourse. *Hydrological Processes* **29**: 3423-3440. DOI:

483   10.1002/hyp.10457.

484   Verma MP, Portugal E, Gangloff S, Armienta MA, Chandrasekharam D, Sanchez M,

485   Renderos RE, Juanco M, van Geldern R. 2015. Determination of carbonic species

486   concentration in natural waters - Results from a worldwide proficiency test.

487   *Geostandards and Geoanalytical Research* **39**: 233-255. DOI: 10.1111/j.1751-

488   908X.2014.00306.x.

489   Wippern J. 1955. *Erläuterungen zur Geologischen Karte von Bayern 1: 25000 - Blatt Nr.*

490   *6134 Waischenfeld*. Bayerisches Geologisches Landesamt; 47.

491   Yang C, Telmer K, Veizer J. 1996. Chemical dynamics of the "St. Lawrence" riverine

492   system: δD_{H2O}, $\delta^{18}O_{H2O}$, $\delta^{13}C_{DIC}$, $\delta^{34}S_{sulfate}$, and dissolved $^{87}Sr/^{86}Sr$. *Geochimica et*

493   *Cosmochimica Acta* **60**: 851-866. DOI: 10.1016/0016-7037(95)00445-9.

494

495 **FIGURE CAPTIONS**

496 Figure 1. Location of the study area in Southern Germany. The total area of the Wiesent

497 Catchment is 1040 km^2.

498

499 Figure 2. Sampling points and lithology of the Wiesent catchment. The upper and central

500 parts of the catchment are dominated by Late Jurassic limestone formations, whereas Late

501 Triassic to Middle Jurrasic claystones and sandstones emerge in the southwestern and eastern

502 part of the catchment that lie further downstream. Sampling points are indicated for the

503 Wiesent main river (numbers in circles) and tributaries (numbers in square boxes).

504

505 Figure 3. Major ion chemistry, electric conductivity (EC), and temperature (T) along the

506 Wiesent River for bi-monthly sampling campaigns. Bicarbonate was calculated from total

507 alkalinity (TA) field titration assuming that TA is comprised by carbonic species only and

508 CO_3^{2-}-contributions are negligible at the observed pH values. Other major ion concentrations

509 were determined by ion chromatography.

510

511 Figure 4. Piper diagram for the Wiesent River and sampled tributaries. Numbers in

512 parentheses refer to sampling locations. The tributaries Truppach (10) and Puettlach (12)

513 mainly drain claystone and sandstone dominated lithology. These tributaries are characterized

514 by lower magnesium, increased potassium and higher sulfate concentrations. This different

515 water chemistry could also have been caused by anthropogenic inputs.

516

517 Figure 5. (A) Bicarbonate plotted against calcium plus magnesium concentrations of the

518 Wiesent River expressed in meq L^{-1}. The dashed line indicates the stoichiometric relation of

23

519   carbonate weathering. (B) Chloride versus sodium plus potassium expressed in meq L^{-1}. The

520   dashed line indicates the stoichiometric relationship for salt dissolution.
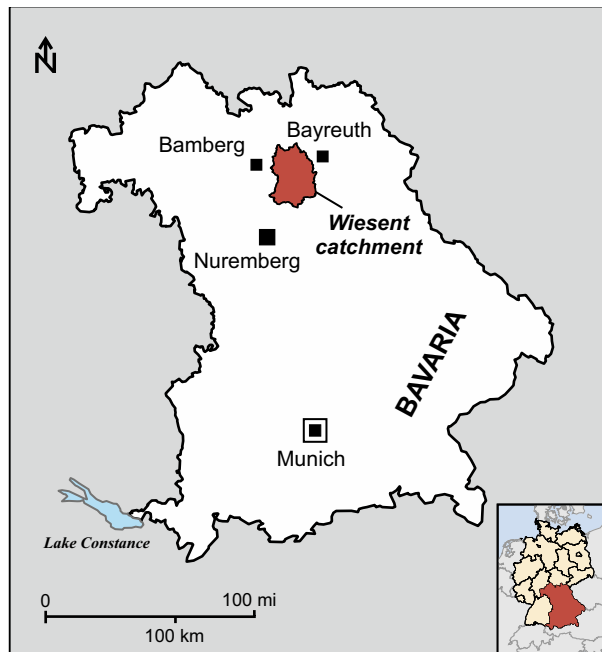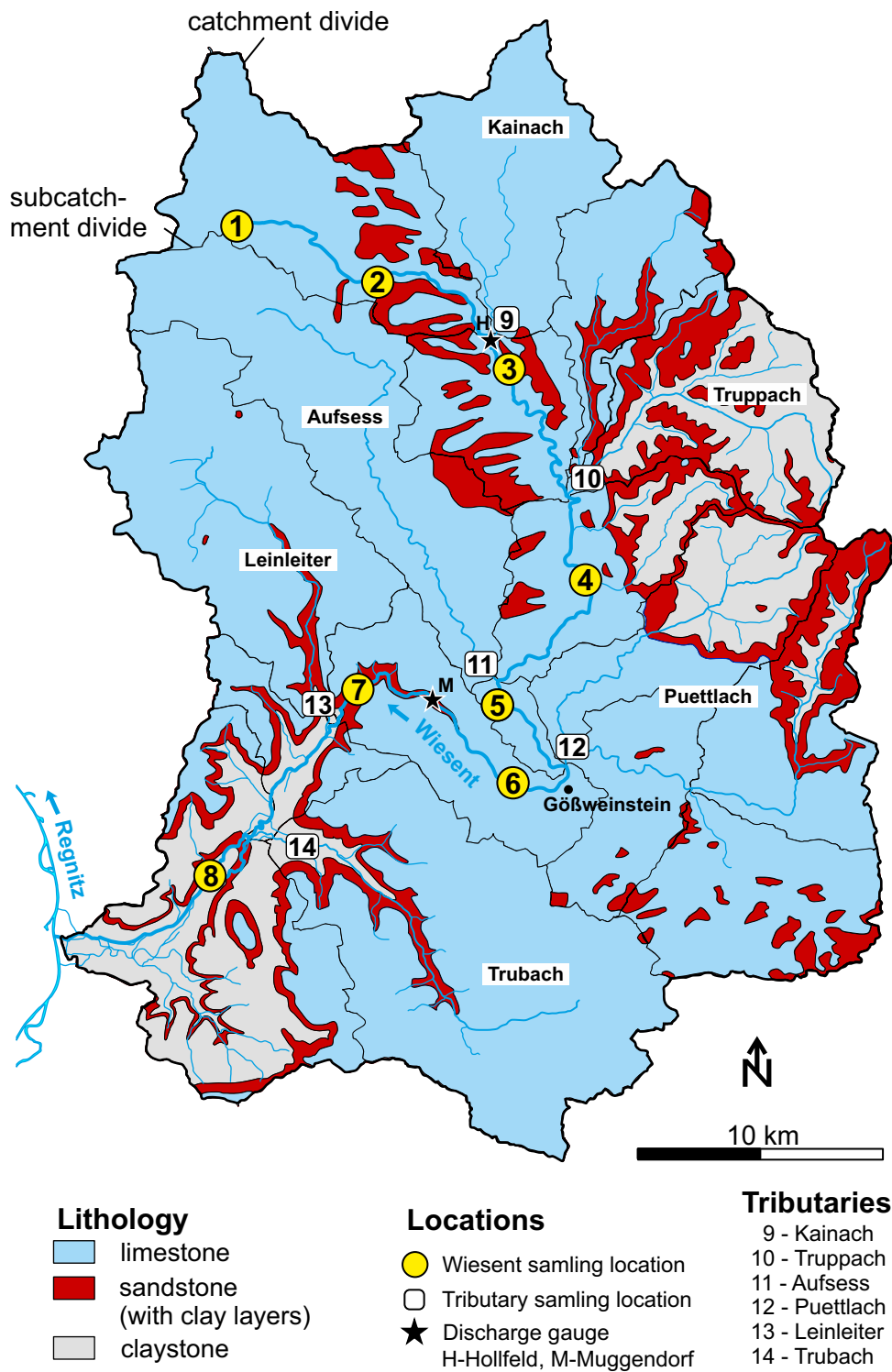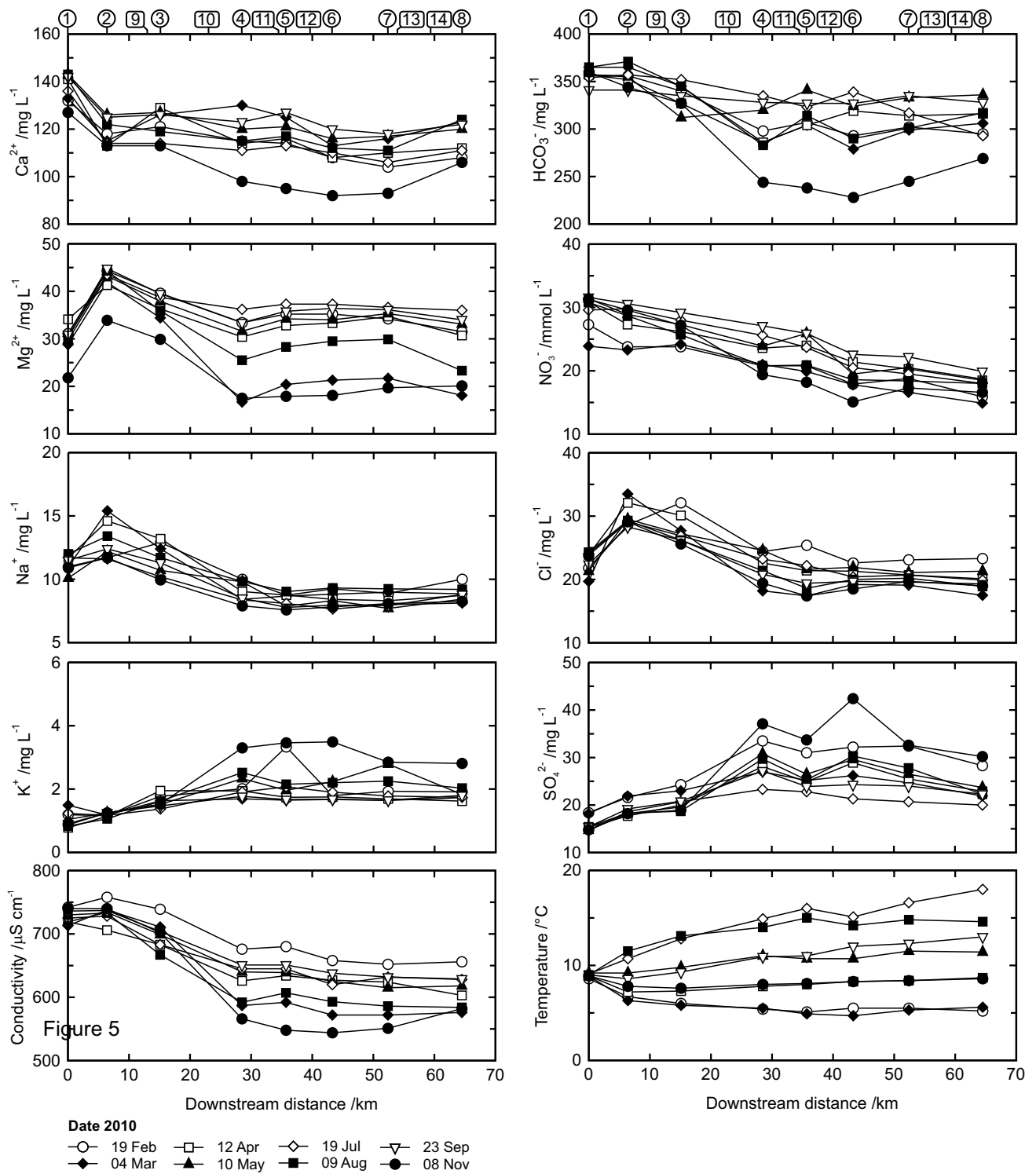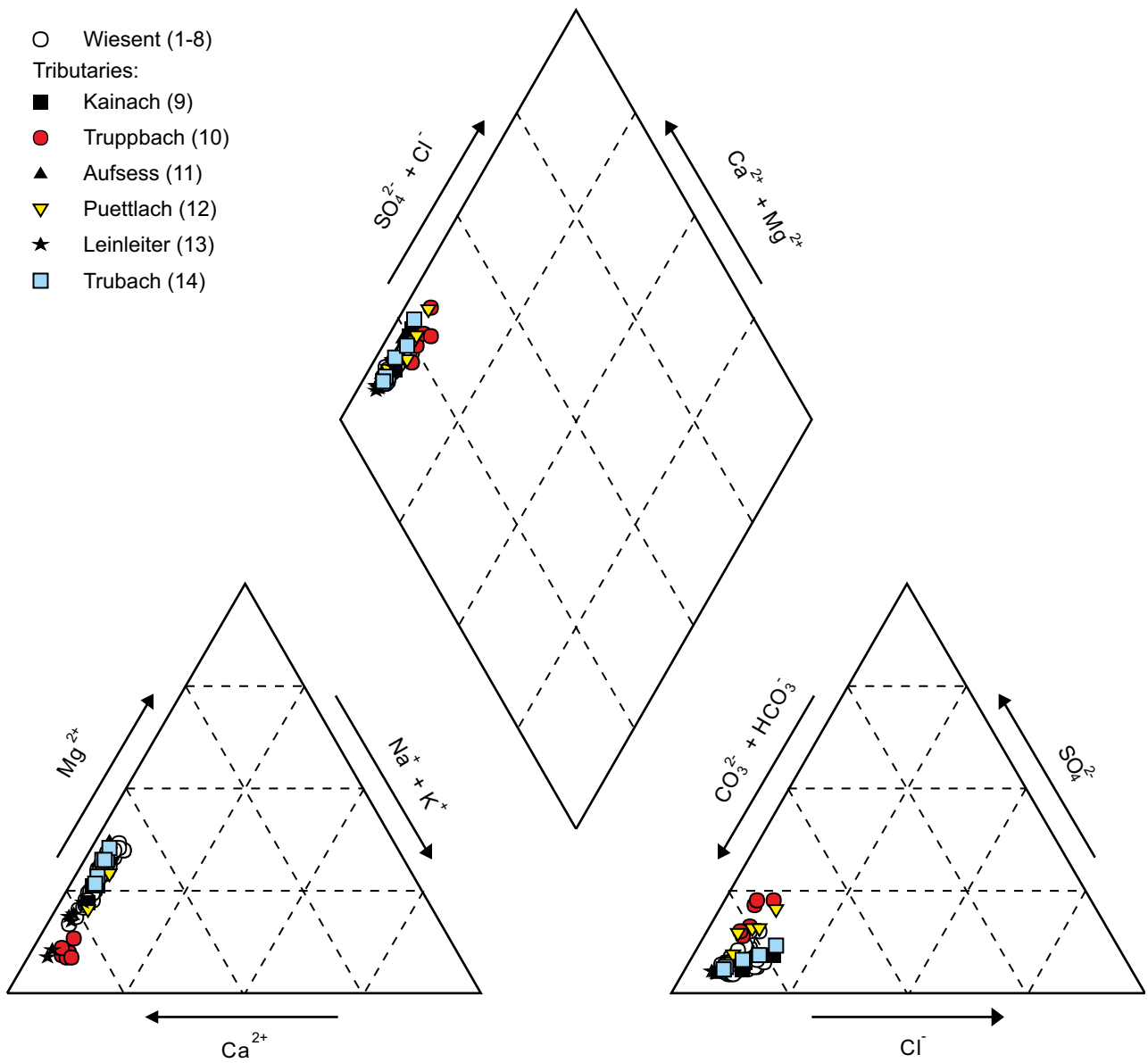
Figure 1

Figure 2

catchment divide

subcatch-
ment divide

Kainach

H 9

Truppach

Aufsess

10

Leinleiter

11

13 7

M

5

Puettlach

12

Wiesent

6

Gößweinstein

8

14

Regnitz

Trubach

N

10 km

Lithology

limestone

sandstone
(with clay layers)

claystone

Locations

Wiesent samling location

Tributary samling location

Discharge gauge
H-Hollfeld, M-Muggendorf

Tributaries
9 - Kainach
10 - Truppach
11 - Aufsess
12 - Puettlach
13 - Leinleiter
14 - Trubach

Figure 5

Date 2010
○ 19 Feb   □ 12 Apr   ◇ 19 Jul   ▽ 23 Sep
◆ 04 Mar   ▲ 10 May   ■ 09 Aug   ● 08 Nov

Figure 3

Wiesent (1-8)
Tributaries:
Kainach (9)
Truppbach (10)
Aufsess (11)
Puettlach (12)
Leinleiter (13)
Trubach (14)

$SO_4^{2-} + Cl^-$

$Ca^{2+} + Mg^{2+}$

Mg^{2+}

$Na^+ + K^+$

Ca^{2+}

$CO_3^{2-} + HCO_3^-$

SO_4^{2-}

Cl^-

Figure 4

Figure 5